Budyko framework based analysis of the effect of climate change on watershed characteristics and their impact on discharge over Europe

Julie Collignan[1], Jan Polcher[1], Sophie Bastin[2], Pere Quintana-Segui[3]

[1]Laboratoire de Météorologie Dynamique/IPSL - Ecole Polytechnique/CNRS -, Paris, France
[2]Laboratoire Atmosphères, Observations Spatiales/IPSL - CNRS -, Paris, France
[3]Observatori de l'Ebre (Universitat Ramon Llull – CSIC), Roquetes, Spain

Key Points:

- Evaluate the role of climate change on the evolution of discharge of European rivers.
- Using the Budyko model as a detection tool for changes in hydrological behaviors of watersheds.
- Analyse the effects of changes in the intra-annual distribution of precipitations on the evolution of the annual discharge.

Corresponding author: Julie Collignan, julie.collignan@lmd.ipsl.fr

Abstract

In a context of climate change, the stakes surrounding water availability are getting higher. Decomposing and quantifying the effects of climate on discharge allows to better understand their impact on water resources. We propose a methodology to separate the effect of change in annual mean of climate variables from the effect of intra-annual distribution of precipitations. It combines the Budyko framework with outputs from a Land Surface Model (LSM). The LSM is used to reproduces the behavior of 2134 reconstructed watersheds over Europe between 1902 and 2010, with climate inputs as the only source of change. We fit to the LSM outputs a one parameter approximation to the Budyko framework. It accounts for the evolution of annual mean in precipitation (P) and potential evapotranspiration (PET). We introduce a time-varying parameter in the equation which represents the effect of long-term variations in the intra-annual distribution of P and PET. To better assess the effects of changes in annual means or in intra-annual distribution of P, we construct synthetic forcings fixing one or the other. The results over Europe show that the changes in discharge due to climate are dominated by the trends in the annual averages of P. The second main climate driver is PET, except over the Mediterranean area where changes in intra-annual variations of P have a higher impact on discharge than trends in PET. Therefore the effects of changes in intra-annual distribution of climate variables are not to be neglected when looking at changes in annual discharge.

Plain Language Summary

Water availability is a high stake for all societies. Different competing activities rely on that resource and its scarcity challenges social, economical and environmental conflicts. With climate change, river discharge and more generally the full water cycle is impacted. Furthermore, many human activities such as dams and irrigation concurrently change the balance of the water cycle over watersheds. Which is the impact of climate change on discharge? How to separate the effect of climate change from the effect of direct human activities? Models are a way to represent reality with an understanding of the physical phenomena included. They can be used to represent the behavior of watersheds without human intervention. We develop a methodology to highlight the climate factors impacting discharge. It compares the impact of changes in seasonality to changes in annual averages of climate variables. We find that annual discharge changes are mostly driven by changes in annual precipitation over Europe. The increasing temperature leads to increasing evaporative demand and is the second most impacting factor over most of Europe. However, over the Mediterranean area where water is more limiting, changes in the seasonality of precipitations has a higher impact than changes in the evaporative demand.

1 Introduction

Water is a key resources for all societies and both its excess and its scarcity can lead to challenging economical, environmental and social issues. Understanding the hydrological cycle and how it evolves due to a changing climate is a major challenge of the century. If we focus our analysis on past changes over Europe, the atmospheric demand for moisture (PET) has been raising, along with modifications of precipitations (P). The observed changes in P show that not only the annual average of P is changing but there are differences in these changes between Summer and Winter, dependent on the area (Zveryaev, 2004). Over Europe, Christidis and Stott (2022) showed that the Mediterranean area tends to become dryer while the rest of Europe becomes wetter over the past century, with weaker relative trends in Summer than in Winter. Therefore it is important to not only look at the effects of changes in the annual averages of climate variables but also to look at the effect of changes in seasonality and intra-annual distribution of these vari-

ables. The distribution of P within the year and its coupling or decoupling from the atmospheric demand PET will influence the partitioning of water between evapotranspiration and runoff at the annual scale.

Changes in the different climate variables governing the water cycle will evidently change equilibriums in the water balance over the different watersheds, impacting the discharge of rivers. Milly et al. (2005) showed that streamflow trends world wide are and will continue to be significantly impacted by changes in climatic factors. Studies show the impact of distribution and concentration of rainfall events on peaks of discharge Q (Tuel et al., 2022). However rivers are also highly managed and human activities are a main driver of change in the functioning of watersheds. The main difficulty in analyzing the effect of climate is to decompose the effects of the different drivers of change on discharge and isolate the effect of climate to better understand its relative importance. Our goal in this study is to propose a tool which can decompose and analyze the sensitivity of discharge to climate change and separate it from internal watershed changes.

Physical based hydrological and Land Surface Models (LSM) are getting more and more complex, able to reproduce the behavior of watersheds and to model discharge. However due to that complexity, it is more difficult to decompose the effects of individual climate factors and to interpret their outputs. Other types of models are simpler, dependent on fewer variables, such as statistical models. These later models are more empirical and their elaboration is often limited by the available data. They can't always relate to physical phenomena due to their simplicity. Our methodology combines both types of models to benefit from both the performance and complexity of the physical based model and from the simplicity of analysis of the more empirical model.

The empirical framework we chose to work with is the Budyko framework. It is well-known and widely used in hydrological studies. It relies on the annual mean of the water and energy balance at the scale of a watershed (Tian et al., 2018), taking into account the water and energy limitations of the physical system. This framework relies on the hypothesis that each watershed is at an equilibrium and introduces an empirical parameter which encompasses the watershed characteristics and its evaporation efficiency. The main limitation is that the empirical parameter fitted on discharge observations doesn't distinguish between the concurring effects of climate change and human activities. Furthermore these effects tend to change the annual evaporation dynamics of watersheds and the equilibrium of the system on which the framework relies. The present study introduces a time-moving window to fit the Budyko framework to better capture the effect of climate change and this transition of the equilibrium state.

To focus on the effects of climate change, the present study applies the Budyko framework to outputs of a state of the art LSM. The LSM represents the physical behavior of watersheds and the only source of change introduced in the dynamics of the modeled watersheds is the evolving climate variables applied to the models. The use of LSM outputs also allows to play with the climate parameters to better separate the effects of the different elements of climate change (changes in annual averages against changes in intra-annual distribution of climate variables).

This article is structured as follows: we first present the Budyko framework with its underlying hypothesis and limits. Then we explain the methodology we developed to apply it to the chosen LSM. Synthetic forcings are created to test if our methodology allows to analyse the effects of different aspects of climate change. We explain the use of the time-moving window to look at temporal trends in the different climatic effects. Finally we explain the results obtained over Europe of the effect on discharge trends over the past century of the different element of climate change (changes in annual averages against changes in intra-annual distribution of climate variables).

2 The Budyko framework

2.1 General presentation

Over watersheds which can be considered as closed systems, the water balance equation (1) applies to explain the equilibrium between the variables of the hydrological cycle: the river discharge (Q), the evapotranspiration (E), the precipitation (P) and the change in the water storage over the watershed between two time steps (ΔS).

$$P - \Delta S = Q + E \tag{1}$$

Long-term, ΔS can be reasonably considered as negligible. Ideally, this hypothesis should be applied over a period long enough that the equilibrium of the system is reached (L. Zhang et al., 2008). This also supposes no external perturbations impacting the water budget such as groundwater mining or water transfers to or from other basins.

This hypothesis can be applied over time series of yearly resolution (hydrological year) or coarser, so we can be freed from seasonal variations of the water storage. For the region considered, the hydrological year starts in September, at the end of the dry season, when the reservoirs are supposedly filled at their lowest, to minimize the differences in ΔS from one year to another. Later on, unless specified otherwise, the variables P, E and Q represent the annual averages over the hydrological year.

Commonly used in hydrological research to study Q and E, the budyko framework relies on this long-term equilibrium of water balance over a catchment, coupled to the energy balance. It postulates that the partition of annual water budget between runoff and evapotranspiration over a catchment, represented by the evapotranspiration E, is a function of the relative water supply (rainfall P) and the atmosheric water demand (potential evapotranspiration PET) (Tian et al., 2018; Xing et al., 2018; Yang et al., 2007). The later depends on both the energy availability and on atmospheric turbulences. Therefore this framework takes into account the water and energy limitations of the system which can't evaporate more than the atmospheric demand allows and more water than the catchment reaches with the source of water (P). Different analytical approximations to this hypothesis (Budyko curves) have been developed, expressing the evapotranspiration rate (E/P) as a function of the aridity index (PET/P) over a catchment (fig. 1).

This framework relies on a closed water budget in time and space and neglects ΔS. So it has to be applied over a closed watershed and fitted on a long-term equilibrium. Therefore it is applied over annual averages at the very least and adjusted over several years to consider a long-term equilibrium and validate the hypothesis on ΔS.

2.2 One parameter equation

Parametric equations were developed, introducing an empirical parameter representing the catchment characteristics. Two of the most widely used are the Fu's equation (2) (Ning et al., 2019; Simons et al., 2020; L. Zhang et al., 2008; Zheng et al., 2018) and the Mezentsev–Choudhury–Yang equation (3) (Luo et al., 2020; Roderick & Farquhar, 2011; Wang et al., 2020; Xing et al., 2018; Xiong et al., 2020). These equations can be found under different names in the litterature such as Tixeront-Fu equation for (2) or Turc-Mezentsev for (3) (Andréassian & Sari, 2019).

$$\frac{E}{P} = 1 + \frac{PET}{P} - \left(1 + \left(\frac{PET}{P}\right)^{\nu}\right)^{\frac{1}{\nu}} \tag{2}$$

$$E = \frac{P * PET}{(P^{\omega} + PET^{\omega})^{\frac{1}{\omega}}} \tag{3}$$

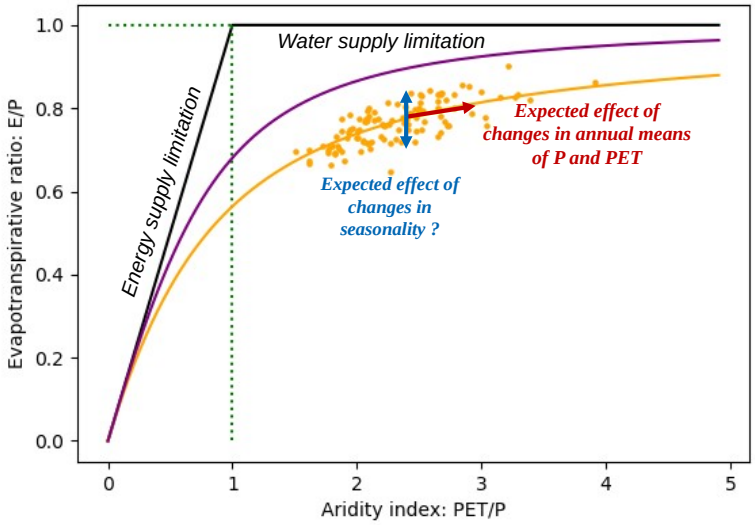

Figure 1. Budyko framework: relationship between evapotranspirative ratio (E/P) and aridity index (PET/P) (Fu's equation). E, PET, P are annual averages. ν associated to the purple curve is larger than ν associated to the orange curve and translate in a higher evaporation efficiency above the watershed. For a given watershed with constant characteristics, there is still a dispersion around the curve of the dots for a given year due to intra-annual variations of the climate cycle (orange dots). The curve and its associated ν represents the average behavior of the watershed. The original framework includes trends in annual climate variables by a displacement along the curve (red arrow). However it doesn't include trends which could impact the way water is partitioned over the catchment such as long-lasting trends in intra-annual distribution of P and PET (blue arrows).

The two parameters derived from equation (2) and (3) are linearly correlated, implying that both equations are almost equivalent (Andréassian & Sari, 2019; du et al., 2016; Roderick & Farquhar, 2011). We examine the sensitivity of the results to the parametric equation used. A limitation exists when fitting Fu's equation for watersheds with a particularly high dryness index such as in arid climates. In these areas, the uncertainty of the estimated ν will increase as the values used to fit the curve are all too close to the plateau (fig 1) and not scattered enough to correctly fit the curve. We fit the watershed parameter ω with Choudhury's equation (3) and a set of E/PET and P/PET. This method ratios to PET gives us a plateau in humid areas as opposed to the previous fit ratioed to P. We obtain very similar results for the methodology with either equation used. We conclude that our area of study is not strongly impacted by this issue and that we could use either equation. For the rest of the study, we use results obtained with Fu's equation (2).

Evapotranspiration (E) measurements are not available over large spatial and temporal scales. Therefore most study work from discharge (Q) analysis. Q can be calculated from the water balance equation (1) where ΔS has been neglected. With Fu's equation (2) used to express E in (1), it yields (4):

$$Q = P * \left(1 + \left(\frac{PET}{P}\right)^{\nu}\right)^{\frac{1}{\nu}} - PET = f(P, PET, \nu) \tag{4}$$

2.3 Discussion of the watershed parameter

The watershed parameter is empirical, calculated by fitting the data over a specific catchment for a given time-period considered to be in an equilibrium state. It determines the shape of the curve. It reflects the various hydrological characteristics of the watershed such as topography, vegetation coverage, soil properties, etc, which play a part in the annual partitioning of water between evapotranspiration and runoff over the catchment.

The original Budyko hypothesis considers a stable equilibrium state of the watershed behavior over the entire period studied. It correspond to a given curve (fig. 1) with a given value of the parameter ν for one watershed. The evolution of climate is taken into account through the evolution of annual averages of climate variables (fig. 1, red arrow). The variability of the annual values (E/P, PET/P) around the fitted curve are due to intra-annual variations of the climate cycle, such as the distribution of rain which changes the covariance between P and PET over the year. For instance, a difference in heavy rain events over a catchment can change the capacity of the soil to store water and change the dynamic of the water partition into runoff and evaporation even if the annual amount of precipitation stays constant. More generally, a change in synchronization between P (water available) and PET (energy demand from the atmosphere) will change E/P for the same average climate (Abatzoglou & Ficklin, 2017; S. Li et al., 2022). In an equilibrium state, the intra-annual variations are supposedly without trends and white noise around that equilibrium. The fitted parameter ν represents the average behavior of the basin.

However watersheds are not always in an equilibrium state. In the various factors characterized with the watershed parameter ν, some can be considered as time invariant (soil type, topography, ...) while others are possibly affected by long-lasting changes. Then the original framework reaches a limit. Furthermore, changes can occur in the hydrological properties of the surface water system, most likely due to direct human intervention such as river management, irrigation, land cover change, while other changes can occur due to climate change or to other climate land surface feedbacks, such as long-lasting changes in heavy raining events and seasonality of climate variables. One difficulty is that these changes are often simultaneous and the framework being semi-empirical, it does not allow to separate these types of changes easily.

Several studies attempt to address these deficiencies. Most studies consider a change between two periods considered as stable, a period of reference and a period post-changes (Jiang et al., 2015; Luo et al., 2020; Wang et al., 2020; Zhao et al., 2018; Zheng et al., 2018) and fit the parameter independently over each period. They obtain two different curves (fig. 1) with two different watershed parameter characterizing the two different equilibrium state before and after change. As a first hypothesis, they then consider that changes in the parameter are only due to anthropogenic changes. Assuming ν to be climate invariant, the changes due to climate is taken into account in the framework only through the changes of the average P and PET (fig. 1, red arrow). Such method neglects the potential effects of climate, such as evolution of seasonality of climate variables, on the evolution of watersheds behaviors reflected by the watershed parameter (fig. 1, blue arrows).

In a second type of attempt, several studies developed an expression of the watershed parameter as a function of significant factors. This would allow to express the evolution of ν over time and decompose the effects of climate and human activities through the different factors chosen. Different methods such as step-wise regressions, neural network were used to identify pertinent factors. However it requires to have enough information on the factors chosen and strong hypotheses stand behind the expression. Ning et al. (2019); Tian et al. (2018); D. Li et al. (2013); S. Li et al. (2022); Xing et al. (2018); X. Zhang et al. (2019), constructed their function across several basins, accounting for

spatially different human, climate and land characteristics. Environmental factors such as soil moisture, seasonality of P and PET, aridity index (S. Li et al., 2022; Ning et al., 2019), vegetation fraction and routing depth (Gentine et al., 2012; D. Li et al., 2013; Ning et al., 2019), relief ratio, drought severity index, seasonality of P and synchronicity between P and PET (Xing et al., 2018) were selected depending on the study. Direct human factors considered were irrigated area (Tian et al., 2018) or water applied for irrigation (D. Li et al., 2013), land use and land cover change in highly managed areas (Tian et al., 2018) or even GDP per capita (X. Zhang et al., 2019). Other factors were tested but not selected, some selected in some studies but not in others, showing the high dependence of the final expression on the choice of factors tested and on the area of study. One strong hypothesis is then that such a relationship defined over spatial differences is also applicable to explain temporal differences (Luo et al., 2020).

Other studies (Jiang et al., 2015; Zhao et al., 2018) looked at time-varying human activities and climate change to construct expressions over time, using a time-moving window to fit the evolution of the catchment parameter over a basin. Factors chosen were temperature, PET and irrigated areas (Jiang et al., 2015). This approach faces another limitation due to the availability of information on the time evolution of the different factors. Ning et al. (2019) used a mixed technique, applying their fit across 30 basins at different time scales using moving time-windows and found that the impact of vegetation cover and climate seasonality on the watershed parameter was stronger over longer time steps.

3 Methodology

The methodology proposed here uses the Budyko framework to explore the sensitivity of discharge to climate change. It focuses on the parameter ν and attempts to decompose its dependence on climate. We want to explore the climate dependence of ν, without having to express it directly. We use the output of a Land Surface Model to reproduce the behavior of watersheds with constant characteristics, subjected to climate change but no other source of change. We develop a time varying $\nu(t)$ to capture part of the change in the behavior of the watersheds due to climate. We compare its effects to the magnitude of change in discharge already captured with the traditional framework which only considers changes in annual averages of P and PET.

3.1 Simulations with a Land Surface Model (LSM)

To isolate the effect of climate change from other factors which could affect watersheds, we work with outputs of a Land Surface Model (LSM). The model constructs watersheds with constant hydrological properties and represents an idealized watershed, without any direct changes from human intervention and other non climatic perturbations. Therefore the only source of long-term change would be due to a difference in response to an evolving climate.

3.1.1 A "natural reference" simulation

In this study, we use the LSM Organizing Carbon and Hydrology In Dynamic Ecosystems (ORCHIDEE) from the Institut Pierre Simon Laplace (IPSL). It includes biophysical and biogeochemical processes to simulate the global carbon cycle and quantify terrestrial water and energy balance. It can be run coupled to an atmospheric model or in off-line mode. In that latter case, the atmospheric conditions are forced by an independent dataset. In the following, we will use the model in stand-alone conditions, with the forcing dataset GSWP3 which covers 1901 to 2013 (Hyungjun, 2017) with a resolution of 0.5°for all climate variables. The hydrological network of the ORCHIDEE LSM is constructed from the hydrological elevation model HydroSHEDS (Lehner et al., 2008) which

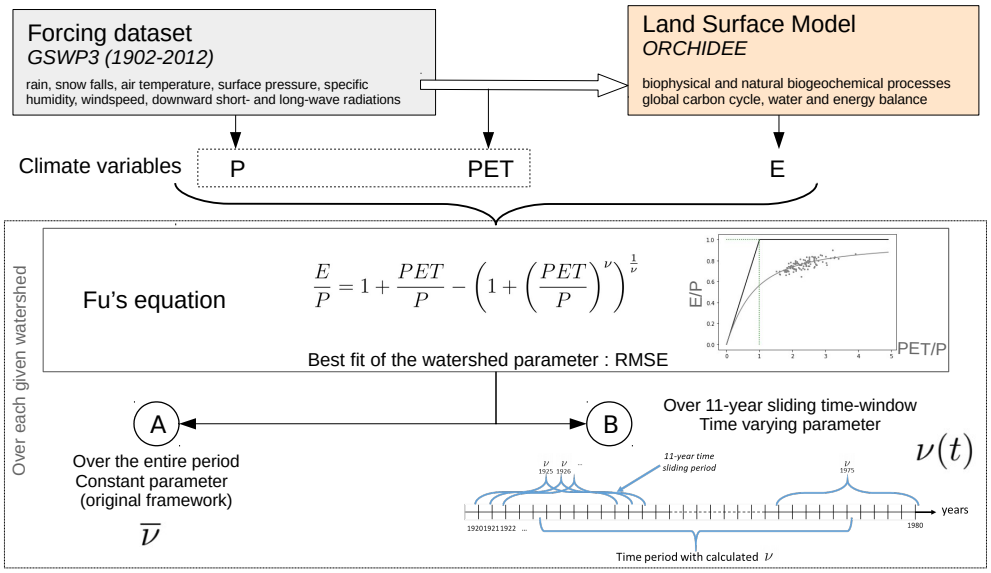

Figure 2. Scheme of the method: The Land Surface Model (LSM) is forced with the forcing dataset to calculate E. The LSM is considered to represent the "climatic reality" over a catchment, without any changes in the watershed characteristics. We then average P, PET and E and integrate it over each watershed to get annual averages for all catchments. Then we fit Fu's equation. A) The fit of the equation over the entire century results in the calculation of an empirical parameter $\overline{\nu}$ which represents the average catchment characteristics. B) To have an evolution of $\nu(t)$ over time, the fit was in a second time applied successively over an 11-year sliding time-period.

covers the area studied with the resolution of 30 arc seconds (approximately 1 kilometer at the equator). The hydrological information is then upscaled to the resolution of the atmospheric grid, the hydrological coherence being preserved by the construction of Hydrological Transfer Units (HTU) at the sub-grid level (Polcher et al., 2022). From a database of gauging stations, upstream basins are reconstituted on the hydrological elevation model grid and then projected on the atmospheric grid during the process. We have access to 2134 stations over the area studied for which the LSM calculates a discharge and for which we have the reconstituted upstream basin.

We consider that the final product correctly reproduces the hydrological network and the water partitioning over a watershed due to climatic phenomena. The modeled watersheds have fixed constant land surface characteristics which will react to the climate data input at each time step (30 min time step). Therefore the LSM output depend on both the evolving annual average and the evolving distribution over the year of the climate variables.

The watershed parameter of the Budyko curve is calculated over each catchment with a fit of the equation curve $E/P = f(PET/P)$ (equation 2), using the minimum root mean square error (RMSE) for a given set of annual averages of evapotranspiration E, precipitation P and potential evapotranspiration PET data (Jiang et al., 2015; Yang et al., 2007).

The climatic variables defining P and PET are from a forcing dataset, GSWP3 here. P is the sum of rainfall and snowfall. PET is calculated through Penman-Monteith

Table 1. Synthetic forcings created

	Forcing name	Average P	Intra-annual variation of P	Description[a]
1	*ref*	-	-	Reference forcing: GSWP3 (1901-2012)
2	*f2000*	fixed	fixed	P has been entirely fixed for each year, equal to the precipitation and the seasonality of the year 2000.
3	*cstmean*	fixed	-	Only the average value of P has been fixed for every year to the one of year 2000
4	*cstintravar*	-	fixed	Only the intra-annual variations of P have been fixed for every year to the one of year 2000

[a]For forcings 2 to 4, P has been modified compared to the reference: the average value of P over the year and/or the distribution of precipitations over the year have been fixed for each year to the value of the year 2000.

equation applied at a 30 min time step (Barella-Ortiz et al., 2013). E is the output of the LSM forced with the same forcing. The gridded outputs (PET, E) are at the resolution of the forcing dataset (0.5°). Then we consider the annual mean P, PET and E over hydrological years, integrated over each catchment. The catchments' shape has been reproduced at finer resolution and then projected on the 0.5°grid.

We fit the parameter once with all points over the entire time period covered by the climate dataset to get $\overline{\nu}$ representing the average behavior for each catchment (fig. 2, A).

3.1.2 Synthetic forcings to analyze the effect of variation of seasonality

In order to better understand the effect of inter and intra-annual climate variations on the Budyko framework and on discharge Q, we constructed synthetic climate forcings. To separate the effect of changes in annual averages of climate variables from the effect of changes in the intra-annual covariance of P and PET, we constructed synthetic forcings fixing one or the other.

The calculation of PET is based on Penman-Monteith equation applied at a 30 min time step (Barella-Ortiz et al., 2013). It includes many related climate variables and non-linear relationships, making it very difficult to anticipate how a change in a given climate variable may influence its behavior. It was therefore too complicated create synthetic forcings for which we would modify climate variables in order to fix PET seasonality for instance. Therefore we only modify the precipitation P in the synthetic forcings, to see how it impacts our results compared to the reference forcing.

The reference forcing is the GSWP3 dataset from September 1901 to September 2012 (3h time step). Then we constructed three forcings which were modified over hydrological years (table 1, fig. 3a):

- *f2000*: A forcing where all 3h values of P are set to the values of the year 2000 (September 1999 to September 2000) for each year. Therefore all component of P (average and intra-annual variations) are set constant.

- *cstmean*: A forcing for which we keep the relative intra-annual distribution of P of each year but where the average P of each year was set constant. The 3h values of P are scaled so the yearly average over the hydrological year is set to the one of the year 2000 (September 1999 to September 2000).
- *cstintravar*: A forcing for which we keep the annual average of P for each year but where the relative intra-annual distribution of P was set constant. The 3h values of P are set to the values of the year 2000 (September 1999 to September 2000) for each year and then scaled over each hydrological year so the yearly average is set to the one of the corresponding year in the reference forcing.

Fig. 3a shows the resulting annual averages of P, PET, E integrated over a given catchment in southern Spain, along with the average monthly distribution of P over the year for each modified forcing. PET is the same for all forcings. The inter-annual variability of P and E is canceled for *f2000* since the variability of E over that area is mostly linked to P. The inter-annual variability of E for *cstmean* is highly reduced but not completely canceled since it is also dependent on intra-annual distribution of P. For *ref* and *cstintravar*, the average monthly distributions of P shown here are computed over the century. It however varies from one year to another which is not illustrated here. For *f2000* and *cstmean*, the average monthly distribution of P shown here corresponds to the distribution of P over the year 2000 and is the same for each year in these forcings, with just a scaling difference in the forcing *cstmean*. Over that given watershed, it results in a concentration of P over April and October and a particularly dry month of February over every year.

We expect that the Budyko framework will work better to reproduce the LSM output when the variation of intra-annual distribution of P are canceled. Indeed the variability of the annual points (E/P, PET/P) around the curve (fig. 1) should be highly reduced.

3.2 Introducing a time-varying watershed parameter ν

For a watershed with constant hydrological properties (which is the case when we consider modeled watershed in ORCHIDEE), if we consider that ν is independent of climate, it should be time invariant.

However, the intra-annual synchronization of P and PET (or the annual covariance between PET and P) impacts the annual mean of E and Q and the average effect of this synchronization is included in the adjustment parameter ν, which is therefore not completely independent of climate. Through its simple framework, the Budyko model does not cover possible changes at intra-annual time scales which can impact the covariance between PET and P over a year. Therefore long-term changes in seasonality should induce a climatic time dependence, not accounted for in the framework with a constant ν. Considering a time varying parameter should therefore improve the Budyko model to better reproduce E and its climatic evolution.

3.2.1 Fit with a sliding time-window

To get a time varying parameter $\nu(t)$ for each catchment, we do several fits over successive 11-year time-sliding sub-periods (fig. 2, B).

We chose 11 years as the smallest time-length over which we could apply the Budyko framework relevantly, considering than each 11-year sub-period is stationary ($\Delta S = 0$). Tian et al. (2018) found that below than time length the fit of the ν parameter was too unstable to be relevant.

This time-varying $\nu(t)$ should enable to capture the possible long-term (above 10 years) variations in the intra-annual water-partitioning over a catchment. These long-

term changes in the annual covariance between P and PET should be the main climatic factors involved in the climatic dependence of ν. The variations of ν may however not be completely independent of the annual averages of P and PET. Crossed effects between annual averages and intra-annual distributions would also be captured into ν variations. For instance, a concentration of raining events over a shorter period would increase the runoff (change in intra-annual distribution of P), effect which would be amplified by an increase of the total amount of water rained (change in annual average of P).

3.2.2 Decomposing the impact of climate on discharge trends

The watershed parameter ν is a conceptual variable providing little insight into the magnitude of discharge changes. We thus examine the impact of $\nu(t)$ changes on the river discharge Q and compare the impact of these changes to the impact of annual averages of climate variables (P and PET) changes on Q over time. We gather P and PET in a "climate" variable $C = (P, PET)$ to simplify the discussion.

Following our previous hypothesis (equation 4), Q can be estimated with the Budyko framework using C and ν: $Q = f(C, \nu(t))$.

Q can be decomposed with first order partial derivatives (equation 5), with the first term of the right hand side, representing the partial derivative due to climate variables C and the second term for the partial derivative due to changes in the watershed parameter $\nu(t)$. We then estimate the partial derivatives due to C and due to ν independently.

$$\frac{dQ}{dt} = \frac{\delta Q}{\delta C}\frac{dC}{dt} + \frac{\delta Q}{\delta \nu}\frac{d\nu}{dt} \qquad with \quad C = (P, PET) \tag{5}$$

To independently estimate the partial derivative due to climate variables C, we need to cancel the second term. To do so, we calculate the discharge $Q_c = f(C, \overline{\nu})$, with a constant value of ν. The trend of that discharge $\frac{dQ_c}{dt}$ matches the term with the partial derivative due to C in equation (5).

To estimate the partial discharge trend due to $\nu(t)$, we need eliminate the trends in annual averages of P and PET over the century to cancel the first term. We randomly draw P and PET pairings for each year. We do so several times and average the results for each year. It gives us a random climate without trends over the century. We then apply Fu's equation (2) with the resulting random annual averages of P and PET and the time varying $\nu(t)$ calculated with the forcing before the random drawing. It gives $Q_\nu = f(C_{rand}, \nu(t))$ for which the climate trends are only due to variations captured by the time varying parameter $\nu(t)$. The trend $\frac{dQ_\nu}{dt}$ matches the term with the partial derivative due to ν in equation (5). In the end, we get:

$$\frac{dQ}{dt} = \frac{dQ_c}{dt} + \frac{dQ_\nu}{dt} \tag{6}$$

We calculate the trends of each term and their significance using the Mann-Kendall non-parametric test, associated to Thiel-Sen slope estimator.

This gives us time-series and associated trends for each of the watershed studied. Fig. 3 shows an example for a watershed in southern Spain. Fig. 3a shows the inter-annual variability of annual averages of climate variables P, PET directly calculated from the atmospheric forcing and E modeled by the LSM, for the different synthetic forcings. Over this watershed, E mostly relates to P. Fig. 3b shows the time-varying $\nu(t)$ resulting from the time-sliding window calculation (blue curve), compared to $\overline{\nu}$ calculated with one fit over the entire century (dashed purple line), for the reference forcing. The bottom plot

(a) Watershed. The colors show the share of the grid point within the watershed. Yellow points are completely within it while bordering grid points are red.
Modified forcings over a given basin: the first row of graphs shows the inter-annual variability of P, PET and E for each forcings. The second row shows the average seasonal distribution of P over the catchment for each forcings over the entire century. The average monthly distributions of P shown here are computed over the century. It however varies from one year to another for the reference forcing and the forcing *cstmean* which is not illustrated here.

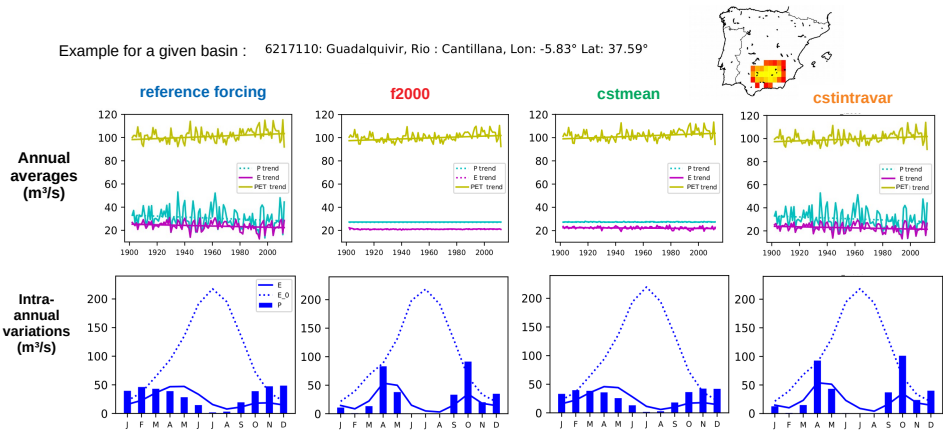

(b) Watershed parameter $\overline{\nu}$ fitted over the entire time period (dashed purple line) and $\nu(t)$ fitted successively over a sliding 11-year time-window (blue line) for the reference forcing.

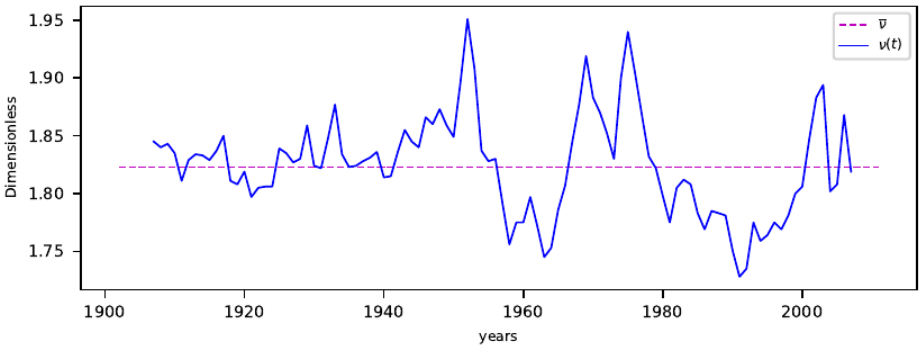

(c) Discharge estimated with Budyko for the reference forcing: $Q = f(P, PET, \nu(t))$ (blue line), $Q_c = f(P, PET, \overline{\nu})$ (purple line), $Q_\nu = f(P_{rand}, E_{0rand}, \nu(t))$ (black line) with their associated trends. Unsignificant trends are dashed. Here all trends are significant.

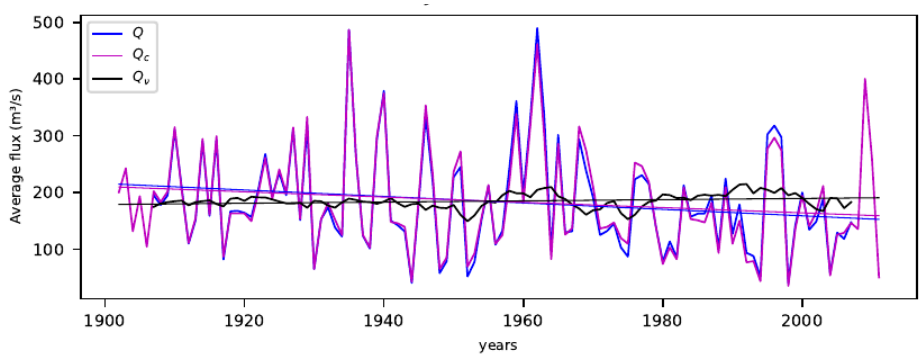

Figure 3. Time series obtained through the full application of our methodology for a given basin

in fig. 3c shows the decomposition of the discharge, comparing the full discharge to partial discharges and their respective trends. The full discharge Q is modeled with the Fu's equation with annual averages of P and PET from the reference forcing and $\nu(t)$. The first partial discharge Q_C is the one calculated without $\nu(t)$ variations. It covers most of Q variations for that given basins. The second partial discharge Q_ν covers some of the missing variations of Q and some of the missing trend. From that figure we can conclude that most variations and trends of the discharge in this basin are explained by $C = (P, PET)$.

4 Results

4.1 Performance of Budyko with or without a time variant ν parameter

Our hypothesis is that for watershed with constant hydrological properties, the dispersion of annual points around the curve is due to intra-annual variations of climate. If these variations did not exist, the original framework should be very close to perfect to model the discharge Q.

To test this hypothesis, we examine the performance of the original Budyko framework with a constant parameter $\overline{\nu}$ to reproduce the discharge from the LSM for the reference forcing compared to the forcing *cstintravar*. For that later forcing, we removed the intra-annual variations of P from one year to another which should improve the performance of the Budyko framework close to perfect if the hypothesis is valid.

We use the Nash-Sutcliffe coefficient (NSC) as performance indicator (equation (7), fig. 4). We consider a NSC$>$ 0.5 to be satisfactory (Moriasi et al., 2007).

$$NSC = 1 - \frac{\sum_{i=0}^{years}(Ql_i - Qb_i)^2}{\sum_{i=0}^{years}(Ql_i - \overline{Ql})^2} \left\{ \begin{array}{l} \text{with Ql= dicharge from the LSM} \\ \text{and Qb= Result from the methodology with Fu's equation} \end{array} \right. \quad (7)$$

We obtain NSC values above 0.5 for 89.9% of all 2134 watershed tested for the original Budyko framework (Q_c, calculated with a constant ν) applied with the reference forcing (boxplot on the left, fig. 4). The original framework is therefore already effective to reproduce the annual discharge over watersheds with constant hydrological properties reacting to an evolving climate.

For the forcing *cstintravar*, NSC for Q_c increases to above 0.6 for all watersheds (boxplot on the right, fig. 4). This confirms our hypothesis: the framework is even more effective if there are no intra-annual variations of P from one year to another. Most of the variability not captured by the original framework is therefore due to the intra-annual variability of P and the covariance of P and PET.

When looking at NSC for the framework applied to the reference forcing with a time varying parameter $Q(ref) = f(C(ref), \nu(t))$, we gain up to 0.26 points of NSC for the tested watershed and reach 94.1% of all watersheds with NSC$>$0.5 (boxplot on the center, fig. 4). It doesn't reach the performance of Q_c with the forcing *cstintravar* but enables to capture some of the variation due to intra-annual trends of climate variables. The part captured are long-term trends due to our choice of the 11-year time moving window. This validates our hypothesis that the introduction of a time varying watershed parameter $\nu(t)$ improves the framework to better encompass climate variability and the effect of climatic trends on discharge, including the effect of climate change on intra-annual distribution and covariance of climate variables (P and PET).

To sum up, most of the inaccuracy of the original framework for watershed with constant hydrological properties are due to variability in intra-annual distribution of cli-

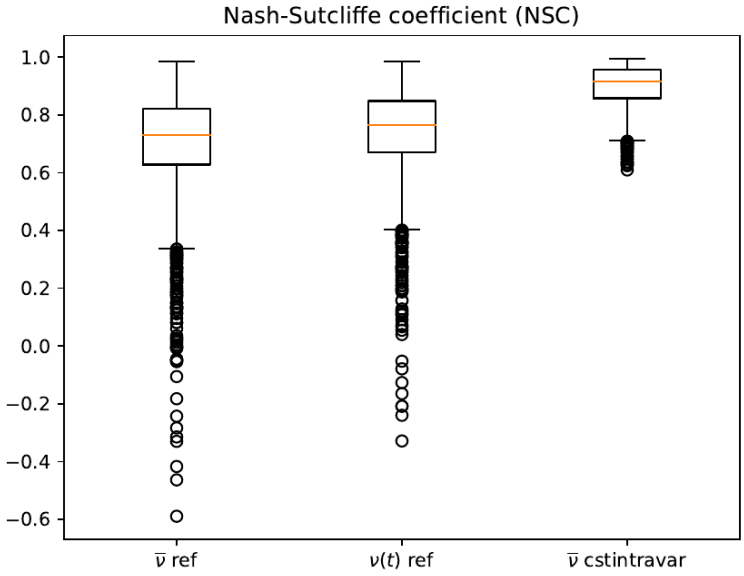

Figure 4. Boxplot of Nash-Sutcliffe coefficient (NSC) over all watersheds: for the forcing of reference with the constant parameter $\overline{\nu}$, with the time varying parameter ν and for the forcing *cstintravar* (where the seasonal distribution of P have been fixed over the entire time period) with a constant $\overline{\nu}$. It represents how well Budyko framework reproduces the discharge output from ORCHIDEE. A value above 0.5 is considered as satisfactory. Very similar results are found when looking at R^2 from a linear regression.

mate variables (P and PET). Our time varying parameter improves the framework by allowing to capture long-term trends in these variations. We now analyze their effect on discharge, compare to the effect of trends in annual average of climate variables.

4.2 Comparing the effects of intra-annual variations of P on discharge Q to the effects of variations in annual averages of P in Europe

We consider our area of study, Western Europe (2134 watersheds modeled) (fig. 7). We first look at the results for the reference forcing for two examples, a basin in England (fig. 5) and a basin in Italy (fig. 6). The discharge obtained through our methodology applied to the reference forcing is the first plot on the top left fig. 5b and 6b. The blue curve represents the full discharge modeled $Q = f(C, \nu(t))$, the purple line the discharge $Q_c = f(C, \overline{\nu})$ with only variations in C accounted for and the black line $Q_\nu = f(C_{rand}, \nu(t))$ with only the variations of $\nu(t)$, mostly changes in the intra-annual covariance of P and PET, accounted for. We represented anomaly of discharge $((Q-Q_{mean})/Q_{mean})$ in order to better compare the plots to each other. For both examples (fig. 5b and 6b), with the reference forcing, the dominant effect in the variations of annual discharge Q (blue line) is due to the annual mean of climate variables C (purple line). Indeed, the blue and the purple curves have very similar variations and trends. We extend the results over all of Europe. Fig. 7a, 7b, 7c show the relative trends over each basins, respectively of Q, Q_c and Q_ν, for the reference forcing. There are significant decreases in the total discharge Q (fig. 7a) (-0.3% to -0.4% per year over the past century) over sparse basins in Spain, the Pyrenees, Italy, Slovenia, Greece and Eastern Europe. There are significant increases (fig. 7a) (+0.2% to +0.4% per year over the past century) over sparse basins in France, Germany, Denmark, Sweden, Northern UK and Serbia. Similarly as for the two examples, these trends are mostly due to changes in the annual averages of

(a) Annual average of climate variables P (light blue line), PET (yellow line) and E (purple line) modeled with the LSM for each academic forcing. Not shown here, the intra-annual distribution of P has been fixed for the forcings *f2000* and *cstintravar*.

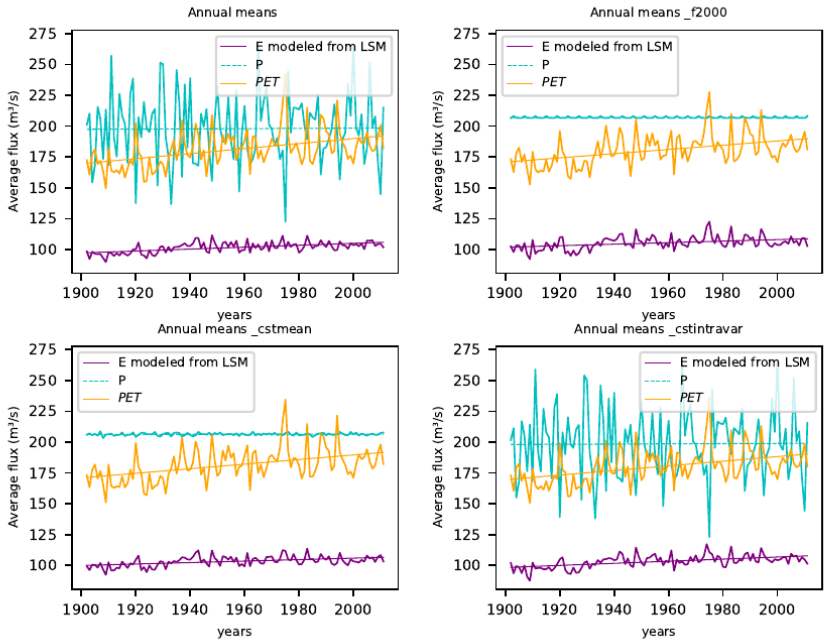

(b) Normalized anomaly of discharge estimated with Budyko: $Q = f(P, PET, \nu(t))$ (blue line), $Q_c = f(P, PET, \overline{\nu})$ (purple line), $Q_\nu = f(P_{rand}, PET_{rand}, \nu(t))$ (black line) with their associated trends. Unsignificant trends are dashed. Here the results for each academic forcing are shown. The scale of the y-axis changes and is divided by 5 for the focings *f2000* and *cstmean*.

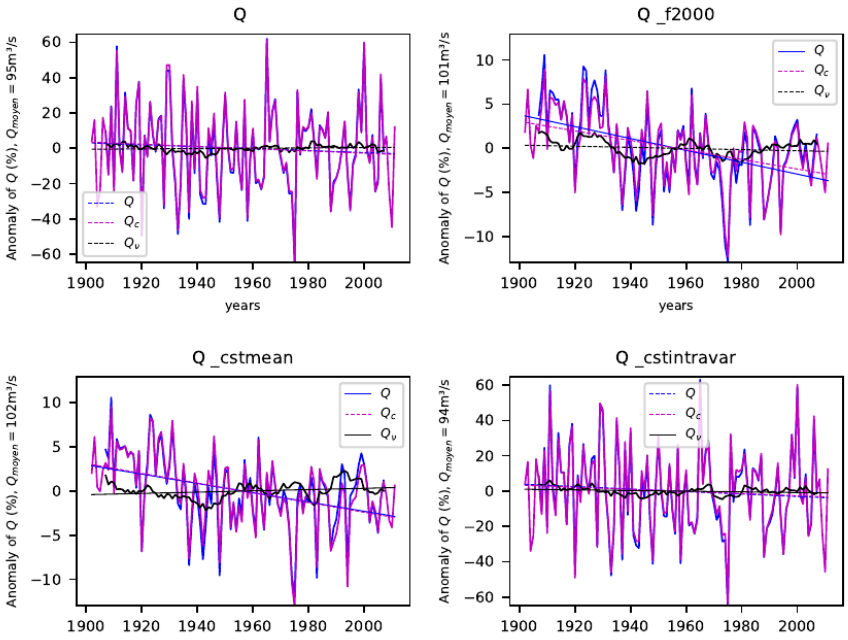

Figure 5. Example 1: Time series obtained through the full application of our methodology for a given basin in England.

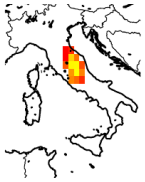

(a) Annual average of climate variables P (light blue line), PET (yellow line) and E (purple line) modeled with the LSM for each academic forcing. Not shown here, the intra-annual distribution of P has been fixed for the forcings *f2000* and *cstintravar*.

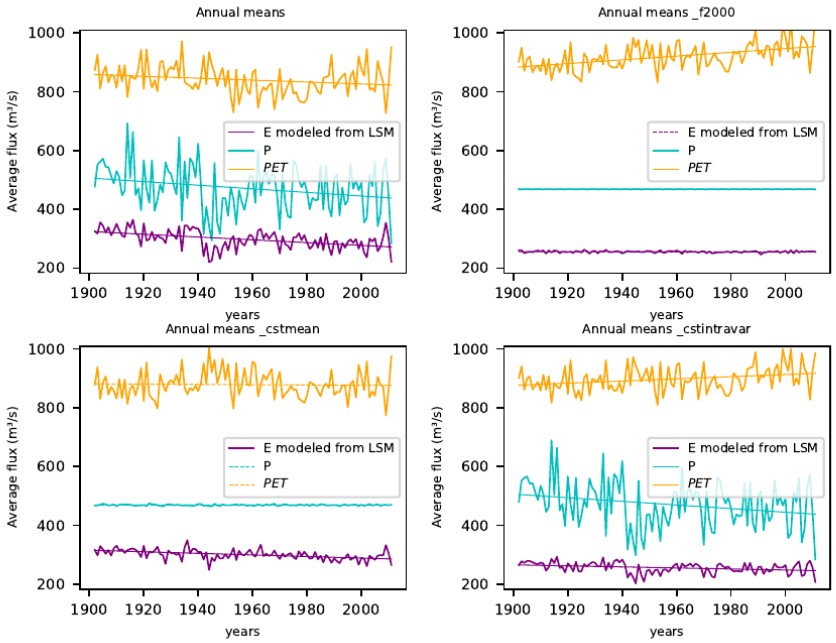

(b) Normalized anomaly of discharge estimated with Budyko: $Q = f(P, PET, \nu(t))$ (blue line), $Q_c = f(P, PET, \overline{\nu})$ (purple line), $Q_\nu = f(P_{rand}, PET_{rand}, \nu(t))$ (black line) with their associated trends. Unsignificant trends are dashed. Here the results for each academic forcing are shown. The scale of the y-axis changes and is divided by 5 for the focings *f2000* and *cstmean*.

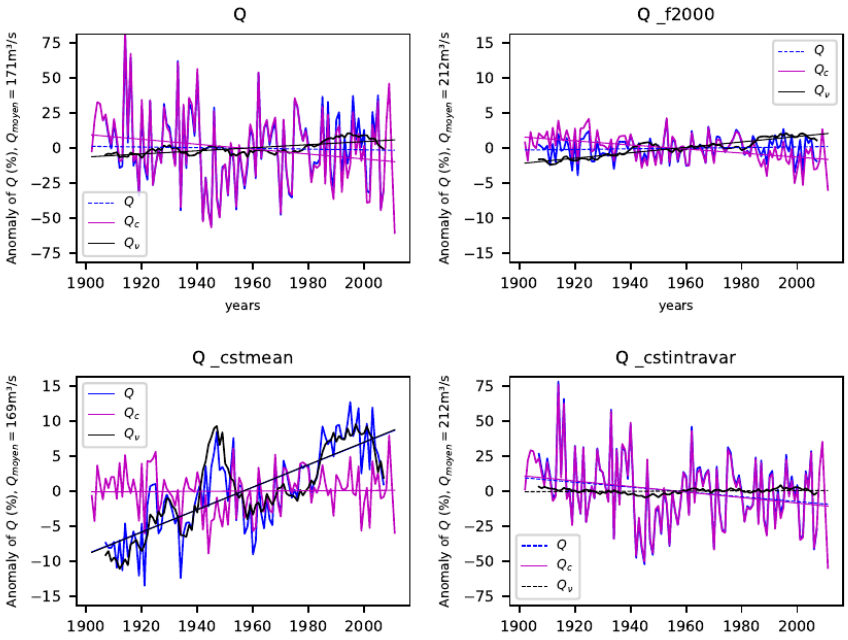

Figure 6. Example 2: Time series obtained through the full application of our methodology for a given basin in Italy.

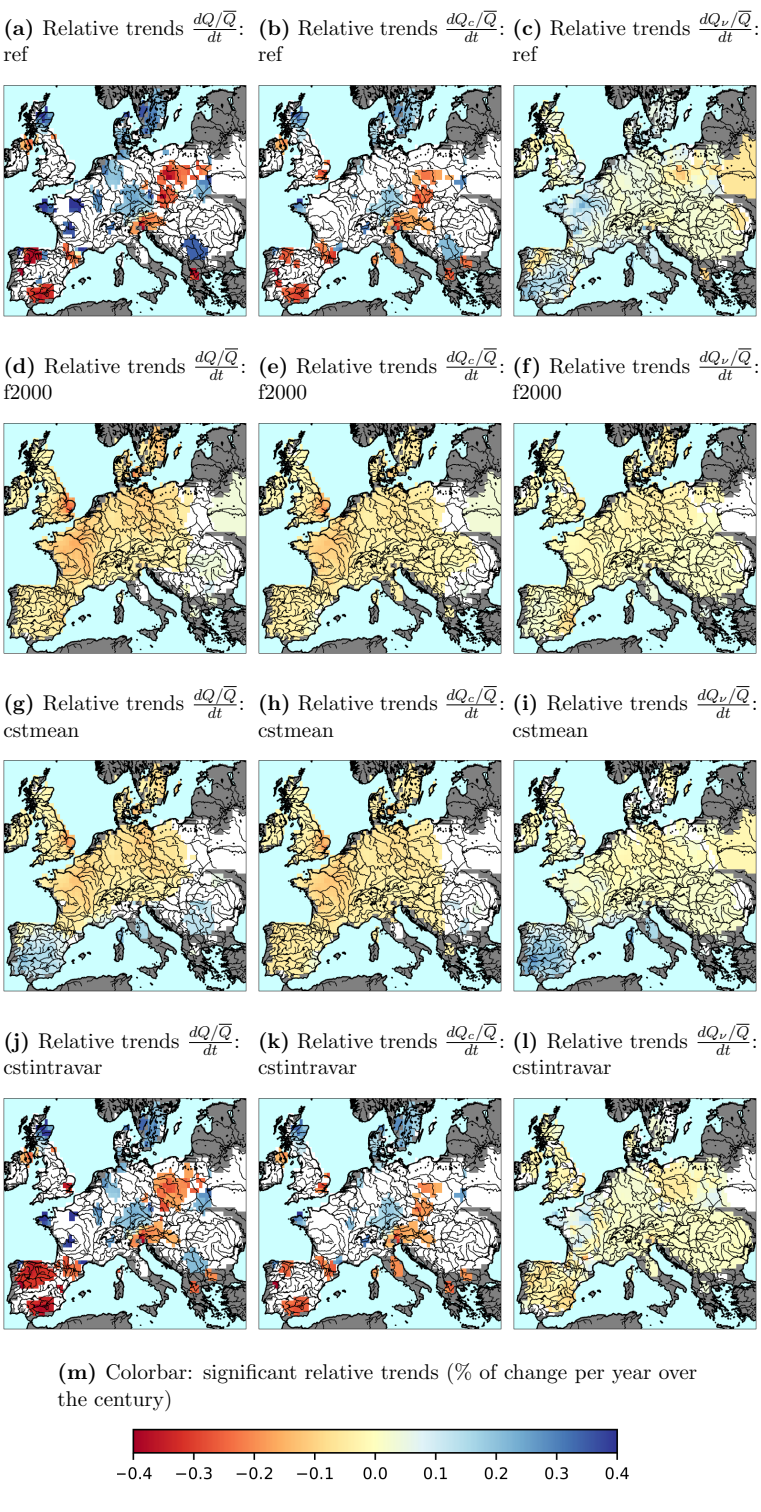

Figure 7. Decomposition of significant relative Q trends (% of change per year over the century) for all the tested forcings: the first line is the reference forcing. The first column is the total change in Q, the second column is the partial change due to trends in annual average of P and PET, the last column is the partial change due to changes in the watershed parameter, mostly due to trends in intra-annual distribution of P and PET. For the modified forcings: $f2000$ has the annual average and intra-annual distribution of P fixed for every year to their value for the year 2000. *cstmean* has only the annual average of P fixed. *cstintravar* has only the intra-annual distribution of P fixed. White areas don't have significant trends.

$C = (P, PET)$ since the Budyko framework with a constant parameter Q_c captures most of it (fig 7b). The inter-annual variability of C is high, making the trends less than 95% significant over most basins for Q and Q_c. Changes in C are the dominant factors explaining the trends in Q over the past century in Europe. This is confirmed by the results obtained with the forcing *cstintravar* (bottom right for fig. 5b and 6b and maps fig. 7j to 7l). It shows that without inter-annual changes in P distribution, in other words, with a maximum reduction of the inter-annual changes in the annual covariance of P and PET, the discharge Q obtained and the associated relative trends are very similar to the results obtained with the reference forcing. Therefore the effects of changes in the covariance of P and PET is minor compared to the effects of changes in the annual mean of climate variables C in most of Europe.

However, there are some areas where the effects of intra-annual distribution of P can't be neglected. If we look at the Tiber river in Italy (fig. 6b), the trend in Q_c is similarly significant for both the reference forcing and the forcing *cstintravar* but the trend in the total discharge Q is only significant for the forcing *cstintravar*. For the reference forcing, the decreasing trend in the discharge due to C (Q_c) is counteracted by the increasing trend due to $\nu(t)$ (Q_ν), making the final trend in discharge Q not significant. More generally over Europe, when we erase the inter-annual variability of C, we capture the effect of trends in the intra-annual distribution of P and PET, through our $\nu(t)$, in Q_ν (fig 7c). It tends to increase discharge especially in the South-West of Spain, Italy and Western France (+0.1% per year over the century). It corresponds to the increasing trend for the black line in fig. 6b, top left graphs for the Tiber river. It has an opposite trend towards decreasing discharge in Eastern Europe and has a rather neutral effect in the rest of Europe (fig. 7c and example of the basin in England fig. 5b, top left graph, black line). This effect is masked in the total trend in discharge by the high inter-annual variability of C (fig. 5b and 6b, top left graphs, blue line). However it amplifies the trends due to changes in annual averages of C over some watersheds such as the Duero basin (North-West of Spain, decrease in discharge), western France and northern Germany (significant increase in discharge over some watersheds where the effect of changes in C alone was not significant). In some other areas, such as for the Tiber river in Italy, or in Southern UK, the effect of intra-annual variability of P and PET counteracts the effect of C, making the relative total Q trends loose their significance due to opposite signals (decreasing trend due to the evolution of C while the effect of change in the intra-annual distribution of the climate variables tend to an increase in the discharge).

To look more closely at the effects of the intra-annual variations of P on discharge, we examine the results for the synthetic forcing *f2000* and *cstmean* (respectively top right and bottom left fig. 5b and 6b and maps 7d to 7f and 7g to 7i).

When we look at the results for the synthetic forcing $f2000$ (fig 7d to 7f), for which P has been entirely set to that of year 2000 for each year, we therefore only get the trends due to changes in PET. For the synthetic forcing *cstmean*, only the annual mean of P has been set, we therefore get the trends due to PET and due to changes in the intra-annual distribution of P.

Free of the high inter-annual variability of the annual mean of P, the trends in discharge are significant over more watersheds for both forcings, with significant trends for 1883 basins with the forcing *f2000* and 1756 basins for the forcing *cstmean* against only 352 basins with significant trends in Q out of 2134 for the reference forcing. However, their magnitude is also a lot smaller. When we compare to the discharge obtained with the reference forcing, it shows that the main factor driving Q is the annual mean of P since when free of its variations, the discharge looks completely different.

For the forcing *f2000*, the effect of PET is towards a decrease in discharge over all of Europe (less than -0.1% to -0.2% per year over the century) (fig. 7d). It is found for both the chosen examples that the effect of PET (top right graphs) tends to decrease

discharge (purple line, Q_c when P has been fixed). It is coherent with the the significant increase in PET (fig. 5a and 6a, top right). The effect of intra-annual variations of PET (fig 7f and black lines, top right graph fig. 5b and 6b) has the same order of magnitude, if not a little smaller (less than -0.1% per year over the century), than the effect of inter-annual change of the annual average of PET (fig 7e or purple line top right graph fig. 5b and 6b). It tends to amplify the effect of the later, especially over Western France and Southern UK and has a slight opposite effect towards increasing trends in Q (less than +0.08% per year over the century) over the East of Europe, West of Spain and for the Tiber river. The effect of changes in annual mean of PET in this specific case is canceled in the total discharge (blue line) by the effect of the changes in the intra-annual distribution of PET captured in Q_ν (black line) (6b).

For the forcing *cstmean*, we now add the effect of changes in the covariance of P and PET due to changes in the intra-annual distribution of P. Depending on the area, there are two different responses. The two basins chosen in example each correspond to one type of response. In the case of the basin in England (Trent river), the results obtained for the forcing *cstmean* (fig. 5b, bottom left) are very similar to the results obtained for *f2000* (fig.5b, top right). It means that the effect due to changes in the covariance of P and PET have little impact compare to the effect of the annual mean of PET over that basin. It matches the results over the North of Europe, especially over France, Germany, South of UK where the trends in Q (fig 7g) are mostly driven by changes in the annual mean of PET (fig 7h). However over the second example of the Tiber river in Italy, the results obtained for the forcing *cstmean* (fig. 6b, bottom left) shows that the changes in the total discharge Q (blue line) match the changes due to the evolution of $\nu(t)$ (Q_ν, black line). In that latter case, the effect of the intra-annual variations of P is dominant to the effect of changes in PET. This matches the results over the South of Europe (Spain, Italy) where for the forcing *cstmean*, the trends in Q (fig 7g) are mostly driven by changes in $\nu(t)$ (fig 7i). These trends are increasing trends in discharge which diverges from the trends due to changes in C in the area (reference forcing and forcing *f2000*, purple lines).

To sum up the results obtained with the synthetic forcings, the annual mean of P is the first driver of change in the annual discharge over all of Europe but its high inter-annual variability tends to hide the trends over most areas. The second most important climatic driver of change in discharge is dependent on the area. Over the South of Europe (Italy, Spain) where water is the limiting factor to evapotranspiration, the second most important climatic factor driving discharge changes is the intra-annual distribution of P. Over the rest of Europe where water is less limiting, the second most important factor driving discharge changes is the increasing PET.

5 Discussion

Several studies have shown the impact of climate change on climate variables over the past century on our area of interest. Annual precipitations increased between 1901 and 2005 over most of Europe but the Mediterranean area where they tend to decrease (Douville et al., 2021; Knutson & Zeng, 2018). Trends per decade are less significant due to the high inter-annual variability of P (Douville et al., 2021). Trends in PET are linked to an increase in the energy available at the surface, highly correlated to the raising temperatures (Douville et al., 2021; Vicente-Serrano et al., 2014). Few studies have directly looked at the trends in PET over Europe, except over the Mediterranean area where studies have shown a significant increase in PET over the end of the century (Vicente-Serrano et al., 2014; Kitsara et al., 2013). The intra-annual variations of climatic variables are more difficult to assess and very little indices exist to measure the inter-annual changes in the distribution of climate variables. García-Barrón et al. (2018) defined indices to assess the evolution over time of the intra-annual cycle of P over the Iberian peninsula. They find that there is a shift over the end of the century of the main rainfall periods

towards autumn, especially over the Atlantic basins and an increase in the inter-annual variability of the intra-annual cycle, especially over the Mediterranean basins.

We look at the trends in P, PET and calculated the indices defined by García-Barrón et al. (2013) to evaluate the trends in the intra-annual cycle of P for the forcing GSWP3. We find that our results concur with those in the literature, validating that this forcing reasonably reproduces the climatic trends of the past century over Europe. The trends in PET are significantly (95% level) increasing over all of Europe. However the trends in P are most often non significant because of its high inter-annual variability, with a significant trend in the annual average of P for 413 catchments out of the 2134 selected. The trends in the intra-annual cycle are also mostly qualitative.

We find in the present study that the main driver of annual discharge Q is the annual mean of P. As expected with the increase in P over western Europe and the decrease in P observed in the Mediterranean area, the trends in Q have a concurring direction.

Our methodology allows to separate the effect of this main driver from secondary climatic parameter which also affect discharge trends. The effects of intra-annual variations of P on discharge are mostly considered in the literature through the study of seasonality and annual extremes of P and PET, to examine their impact on floods (Douville et al., 2021; Rottler et al., 2020; Milly et al., 2002) and drought events (Douville et al., 2021; Vicente-Serrano et al., 2014). However we find that over the Iberian peninsula and the Mediterranean area at least, the effect of the evolution of intra-annual variations of P is the second most important factor impacting the changes in the annual discharge, with a higher effect on discharge than the increase of PET over the century. The intra-annual covariance of P and PET impacts the annual behavior of the catchment and the annual balance between evapotranspiration and discharge since it changes the timing between water and energy availability throughout the year. Therefore intra-annual distribution of P deserves more attention when studying the evolution of annual discharge. The evolution of the intra-annual cycle of P tends towards decreasing discharge in the Mediterranean area. It counteracts partially the effect of decreasing P and increasing PET on discharge. It could be explained by the tendencies of the annual cycle to have an increasingly marked seasonality, concentrating rain events in less but more intense events over the year and thus increasing runoff and relative discharge. Furthermore, our methodology allows to identify these effects despite the only qualitative trends observed in the indices used to measure the intra-annual distribution of P.

Over the rest of Europe where water is less of a limiting factor, the secondary most important climatic factor on discharge changes is PET, which leads to a decrease in discharge due to the increasing evaporative demand by the atmosphere. In the Mediterranean area, PET trends have a lesser impact because the water limit is dominating, being already reached at the end of spring and during all summer. A warmer summer doesn't have therefore a strong impact.

6 Conclusions and perspectives

Similarly to the results of Abatzoglou and Ficklin (2017); S. Li et al. (2022); Xing et al. (2018), we found that the original Budyko framework with a constant watershed parameter $\overline{\nu}$ does not capture climate related changes in the watershed behavior impacting its evaporation efficiency. We have shown that this could be alleviated by introducing a time-dependent parameter $\nu(t)$ which would include the effect of these changes.

Our method doesn't need to define an expression of this $\nu(t)$, which would be highly dependent on the area of study and on the factors available. It can directly be used to estimate the effects over time of changes in the climatic parameter and quantify their relative impacts on discharge trends. To do so we use a time-moving window. The choice

of the window size determines the size of the trends accounted for. It works as a filter of frequency and only captures the effect of variations over periods the size of the window or larger. We had to find a balance between the length of our dataset and the pertinent length of the trends we wanted to analyse. Since we want to look at the effects of climate change, we do not need to capture the high inter-annual variability and can focus on decadal trends or longer. Furthermore, a shorter time window would not be adapted to the hypothesis to the Budyko framework which needs a long enough time-period to be fitted. So the window can't be shorter (Tian et al., 2018). We could test longer time-window to test which is the limit time-length capturing the most impacting effect on discharge. However the longer the time-window, the fewer the points we will have to evaluate the trends.

We apply our modified Budyko framework to LSM outputs to isolate the discharge variations due to changes in climate factors. This methodology relies on the capacity of the chosen LSM to reproduce the "natural" response of a catchment to climate, such as its behavior and response to changes in the intra-annual distribution of P. Our methodology to calculate a time-varying $\nu(t)$ for the Budyko framework, when applied to the output of LSM simulated watersheds with constant hydrological properties, allows to capture the long-term variability of Q due to climate effects not included in the variations of the averages of P and PET.

These changes captured in the time varying $\nu(t)$ are mostly due to changes in the covariance of the intra-annual distribution of P and PET. However the effect of intra-annual distribution of climate variables on discharge is not completely independent from the annual mean of P and PET which can impact the magnitude of the identified trends. This is shown by the slight differences observed in Q_ν between respectively the reference forcing and the forcing *cstmean* (fig. 7c and 7i) and between the forcing *f2000* and the forcing *cstintravar* (fig. 7f and 7l). For each pair of forcings, the intra-annual distribution of P is the same but the inter-annual mean of P differs between the two. The difference observed in Q_ν for each pairing is due to a linked effect between the annual mean and the intra-annual distribution of P. Therefore the amplitude of the effect of intra-annual distribution of P and PET quantified here may depend on the choice of the average P fixed (P from the year 2000 in this study). However the differences are smaller than the identified trends, suggesting that the main conclusions over Europe would not change. When studying specific basins, it could be however interesting to choose specific pairings intra-annual distributions/annual averages of P to construct synthetic forcings, to compare how specific associations combine. When looking at absolute values instead of trends, the choice of the reference year will also play an important part. For instance for the watershed in Italy, the effect of the intra-annual distribution of P of the year 2000 tend to a higher discharge (fig. 6b, bottom left, black line, the intra-annual distribution of the end of the century tend to a higher discharge), explaining that when we set every year to its value for the forcings *f2000* and *cstintravar*, we get a higher average discharge over the entire century (see average discharge, y-axis legend).

Furthermore, we could not simply fix PET or its intra-annual variations in our synthetic forcings due to its non linearity dependence on a number of climate variables. Therefore we could not decompose the effects of PET as easily as for the effects of P, which would be interesting to do especially in the areas where P is less limiting such as in the West of France or in the North of Europe.

The amplitude of the results could also depend on the choice of the model or of the forcing data. We tested the use of other forcing datasets: WFDEI (Weedon et al., 2014), which covers the time period from 1979 to 2010, with the same resolution than GSWP3 and E2OFD (Beck et al., 2017), also covering 1979 to 2010 but at a lower resolution. We also tested the use of another model with another forcing, the model SURFEX (Quintana-Seguí et al., 2020) forced with SAFRAN (Quintana-Seguí et al., 2017), over the Ebro river. It gave very similar results over the overlapping period, with little differences in the sig-

nificance of the trends and their amplitude, showing that the results mostly are dependent on the resolution of the forcing rather than on the forcing or the model used. This validates our methodology to use a LSM as a climatic reference. Again when looking at specific basins, it would be interesting to use higher resolution forcings to get a more accurate picture on the effects of climate change on discharge. We could detail the diversity of behaviors between sub-basins within a given catchment, for instance separating the behavior of upstream sub-basins within mountainous areas from the downstream part of the catchment which could be differently responding to climate change.

If we were to work from observations instead of model outputs, there would be other non-climate related sources of variability such as direct human activities or vegetation changes which would modify the watersheds' behaviors. Our next step is to apply the methodology to quantify these human induced changes and compare their magnitude to those attributed to climate in the present study responses.

7 Open Research

Data availability statement

The forcing dataset GSWP3 used to grid P and other climate data and run the LSM over Europe between 1901 and 2010 in the study is attributed to Hyungjun (2017). It is available upon request via doi:10.20783/DIAS.501.

The Land Surface Model used to calculate $E0$ and model the discharge in this study is the LSM Organizing Carbon and Hydrology In Dynamic Ecosystems (ORCHIDEE) from the Institut Pierre Simon Laplace (IPSL). The Main version used in this study is available upon request on the official website `https://orchidee.ipsl.fr/`.

It relies on the hydrological elevation model HydroSHEDS (Lehner et al., 2008) to construct its routing graphs for rivers and reconstruct the upstream areas of gauging stations placed on its grid. It is available to download from `https://www.hydrosheds.org/`.

The gauging stations positioned on the grid come from a database composed from several sources. The main dataset is the one from the Global Runoff Data Centre (GRDC). It is available to download from `https://www.bafg.de/GRDC/EN/02_srvcs/21_tmsrs/riverdischarge_node.html`. It was completed over Spain with data obtained from the Geoportal of Spain Ministerio (Ministerio de Agricultura, pesca y alimentacion, Ministerio para la transicion ecologica y el reto demografico, 2020) and over France with data from the database HYDRO (Ministere de l'ecologie, du developpement durable et de l'energie) (available on request to `https://www.hydro.eaufrance.fr/`, downloaded in February 2021). In this study, we only used the position of these stations and the associated upstream area to reconstruct meaningful watersheds.

References

Abatzoglou, J. T., & Ficklin, D. L. (2017, September). Climatic and physiographic controls of spatial variability in surface water balance over the contiguous United States using the Budyko relationship. *Water Resources Research*, *53*, 7630–7643. doi: 10.1002/2017WR020843

Andréassian, V., & Sari, T. (2019, May). Technical Note: On the puzzling similarity of two water balance formulas – Turc–Mezentsev vs. Tixeront–Fu. *Hydrology and Earth System Sciences*, *23*(5), 2339–2350. doi: 10.5194/hess-23-2339-2019

Barella-Ortiz, A., Polcher, J., Tuzet, A., & Laval, K. (2013, November). Potential evaporation estimation through an unstressed surface-energy balance and its sensitivity to climate change. *Hydrology and Earth System Sciences*, *17*(11), 4625–4639. doi: 10.5194/hess-17-4625-2013

Beck, H. E., van Dijk, A. I. J. M., Levizzani, V., Schellekens, J., Miralles, D. G., Martens, B., & de Roo, A. (2017, January). MSWEP: 3-hourly 0.25° global gridded precipitation (1979–2015) by merging gauge, satellite, and reanalysis data. *Hydrology and Earth System Sciences*, *21*(1), 589–615. doi: 10.5194/hess-21-589-2017

Christidis, N., & Stott, P. A. (2022, August). Human Influence on Seasonal Precipitation in Europe. *Journal of Climate*, *35*(15), 5215–5231. doi: 10.1175/JCLI-D-21-0637.1

Douville, H., Raghavan, K., Renwick, J., Allan, R., Arias, P., Barlow, M., ... Zolina, O. (2021). Water Cycle Changes. In Climate Change 2021: The Physical Science Basis. Contribution of Working Group I to the Sixth Assessment Report of the Intergovernmental Panel on Climate Change. , 1055–1210. doi: 10.1017/9781009157896.010

du, C., Sun, F., Yu, J., Liu, X., & Yaning, C. (2016, January). New interpretation of the role of water balance in an extended Budyko hypothesis in arid regions. *Hydrology and Earth System Sciences*, *20*, 393–409. doi: 10.5194/hess-20-393-2016

García-Barrón, L., Aguilar-Alba, M., Morales, J., & Sousa, A. (2018). Intra-annual rainfall variability in the Spanish hydrographic basins. *International Journal of Climatology*, *38*(5), 2215–2229. doi: 10.1002/joc.5328

García-Barrón, L., Morales, J., & Sousa, A. (2013, November). Characterisation of the intra-annual rainfall and its evolution (1837–2010) in the southwest of the Iberian Peninsula. *Theoretical and Applied Climatology*, *114*(3), 445–457. doi: 10.1007/s00704-013-0855-7

Gentine, P., D'Odorico, P., Lintner, B., Sivandran, G., & Salvucci, G. (2012, October). Interdependence of climate, soil, and vegetation as constrained by the Budyko curve. *Geophysical Research Letters*, *39*, 19404. doi: 10.1029/2012GL053492

Hyungjun, K. (2017). Global Soil Wetness Project Phase 3 Atmospheric Boundary Conditions (Experiment 1) [dataset]. *Data Integration and Analysis System (DIAS)*, 5. doi: doi:10.20783/DIAS.501

Jiang, C., Xiong, L., Wang, D., Liu, P., Guo, S., & Xu, C.-Y. (2015, March). Separating the impacts of climate change and human activities on runoff using the Budyko-type equations with time-varying parameters. *Journal of Hydrology*, *522*, 326–338. doi: 10.1016/j.jhydrol.2014.12.060

Kitsara, G., Papaioannou, G., Papathanasiou, A., & Retalis, A. (2013, April). Dimming/brightening in Athens: Trends in Sunshine Duration, Cloud Cover and Reference Evapotranspiration. *Water Resources Management*, *27*(6), 1623–1633. doi: 10.1007/s11269-012-0229-4

Knutson, T. R., & Zeng, F. (2018, June). Model Assessment of Observed Precipitation Trends over Land Regions: Detectable Human Influences and Possible Low Bias in Model Trends. *Journal of Climate*, *31*(12), 4617–4637. doi:

10.1175/JCLI-D-17-0672.1

Lehner, B., Verdin, K., & Jarvis, A. (2008). New Global Hydrography Derived From Spaceborne Elevation Data [dataset]. *Eos, Transactions American Geophysical Union*, *89*(10), 93–94. doi: 10.1029/2008EO100001

Li, D., Pan, M., Cong, Z., Zhang, L., & Wood, E. (2013). Vegetation control on water and energy balance within the Budyko framework. *Water Resources Research*, *49*(2), 969–976. doi: 10.1002/wrcr.20107

Li, S., Du, T., & Gippel, C. J. (2022, March). A Modified Fu (1981) Equation with a Time-varying Parameter that Improves Estimates of Inter-annual Variability in Catchment Water Balance. *Water Resources Management*, *36*(5), 1645–1659. doi: 10.1007/s11269-021-03057-1

Luo, Y., Yang, Y., Yang, D., & Zhang, S. (2020, November). Quantifying the impact of vegetation changes on global terrestrial runoff using the Budyko framework. *Journal of Hydrology*, *590*, 125389. doi: 10.1016/j.jhydrol.2020.125389

Milly, P. C. D., Dunne, K. A., & Vecchia, A. V. (2005, November). Global pattern of trends in streamflow and water availability in a changing climate. *Nature*, *438*(7066), 347–350. doi: 10.1038/nature04312

Milly, P. C. D., Wetherald, R. T., Dunne, K. A., & Delworth, T. L. (2002, January). Increasing risk of great floods in a changing climate. *Nature*, *415*(6871), 514–517. doi: 10.1038/415514a

Moriasi, D. N., Arnold, J. G., Liew, M. W. V., Bingner, R. L., Harmel, R. D., & Veith, T. L. (2007). MODEL EVALUATION GUIDELINES FOR SYSTEMATIC QUANTIFICATION OF ACCURACY IN WATERSHED SIMULATIONS. *TRANSACTIONS OF THE ASABE*, *50*, 16.

Ning, T., Zhou, S., Chang, F., Shen, H., Li, Z., & Liu, W. (2019, September). Interaction of vegetation, climate and topography on evapotranspiration modelling at different time scales within the Budyko framework. *Agricultural and Forest Meteorology*, *275*, 59–68. doi: 10.1016/j.agrformet.2019.05.001

Polcher, J., Schrapffer, A., Dupont, E., Rinchiuso, L., Zhou, X., Boucher, O., ... Servonnat, J. (2022, September). Hydrological modelling on atmospheric grids; using graphs of sub-grid elements to transport energy and water. *EGUsphere*, 1–34. doi: 10.5194/egusphere-2022-690

Quintana-Seguí, P., Barella-Ortiz, A., Regueiro-Sanfiz, S., & Miguez-Macho, G. (2020, May). The Utility of Land-Surface Model Simulations to Provide Drought Information in a Water Management Context Using Global and Local Forcing Datasets. *Water Resources Management*, *34*(7), 2135–2156. doi: 10.1007/s11269-018-2160-9

Quintana-Seguí, P., Turco, M., Herrera, S., & Miguez-Macho, G. (2017, April). Validation of a new SAFRAN-based gridded precipitation product for Spain and comparisons to Spain02 and ERA-Interim. *Hydrology and Earth System Sciences*, *21*(4), 2187–2201. doi: 10.5194/hess-21-2187-2017

Roderick, M. L., & Farquhar, G. D. (2011). A simple framework for relating variations in runoff to variations in climatic conditions and catchment properties. *Water Resources Research*, *47*(12). doi: 10.1029/2010WR009826

Rottler, E., Francke, T., Bürger, G., & Bronstert, A. (2020, April). Long-term changes in central European river discharge for 1869–2016: Impact of changing snow covers, reservoir constructions and an intensified hydrological cycle. *Hydrology and Earth System Sciences*, *24*(4), 1721–1740. doi: 10.5194/hess-24-1721-2020

Simons, G. W. H., Bastiaanssen, W. G. M., Cheema, M. J. M., Ahmad, B., & Immerzeel, W. W. (2020, June). A novel method to quantify consumed fractions and non-consumptive use of irrigation water: Application to the Indus Basin Irrigation System of Pakistan. *Agricultural Water Management*, *236*, 106174. doi: 10.1016/j.agwat.2020.106174

Tian, L., Jin, J., Wu, P., & Niu, G.-y. (2018, December). Quantifying the Im-

pact of Climate Change and Human Activities on Streamflow in a Semi-Arid Watershed with the Budyko Equation Incorporating Dynamic Vegetation Information. *Water*, *10*(12), 1781. doi: 10.3390/w10121781

Tuel, A., Schaefli, B., Zscheischler, J., & Martius, O. (2022, May). On the links between sub-seasonal clustering of extreme precipitation and high discharge in Switzerland and Europe. *Hydrology and Earth System Sciences*, *26*(10), 2649–2669. doi: 10.5194/hess-26-2649-2022

Vicente-Serrano, S. M., Lopez-Moreno, J.-I., Beguería, S., Lorenzo-Lacruz, J., Sanchez-Lorenzo, A., García-Ruiz, J. M., ... Espejo, F. (2014, April). Evidence of increasing drought severity caused by temperature rise in southern Europe. *Environmental Research Letters*, *9*(4), 044001. doi: 10.1088/1748-9326/9/4/044001

Wang, W., Zhang, Y., & Tang, Q. (2020, December). Impact assessment of climate change and human activities on streamflow signatures in the Yellow River Basin using the Budyko hypothesis and derived differential equation. *Journal of Hydrology*, *591*, 125460. doi: 10.1016/j.jhydrol.2020.125460

Weedon, G. P., Balsamo, G., Bellouin, N., Gomes, S., Best, M. J., & Viterbo, P. (2014). The WFDEI meteorological forcing data set: WATCH Forcing Data methodology applied to ERA-Interim reanalysis data. *Water Resources Research*, *50*(9), 7505–7514. doi: 10.1002/2014WR015638

Xing, W., Wang, W., Shao, Q., & Yong, B. (2018, January). Identification of dominant interactions between climatic seasonality, catchment characteristics and agricultural activities on Budyko-type equation parameter estimation. *Journal of Hydrology*, *556*, 585–599. doi: 10.1016/j.jhydrol.2017.11.048

Xiong, M., Huang, C.-S., & Yang, T. (2020, June). Assessing the Impacts of Climate Change and Land Use/Cover Change on Runoff Based on Improved Budyko Framework Models Considering Arbitrary Partition of the Impacts. *Water*, *12*(6), 1612. doi: 10.3390/w12061612

Yang, D., Sun, F., Liu, Z., Cong, Z., Ni, G., & Lei, Z. (2007, April). Analyzing spatial and temporal variability of annual water-energy balance in nonhumid regions of China using the Budyko hypothesis. *Water Resources Research*, *43*(4). doi: 10.1029/2006WR005224

Zhang, L., Potter, N., Hickel, K., Zhang, Y., & Shao, Q. (2008, October). Water balance modeling over variable time scales based on the Budyko framework – Model development and testing. *Journal of Hydrology*, *360*(1), 117–131. doi: 10.1016/j.jhydrol.2008.07.021

Zhang, X., Dong, Q., Costa, V., & Wang, X. (2019, May). A hierarchical Bayesian model for decomposing the impacts of human activities and climate change on water resources in China. *Science of The Total Environment*, *665*, 836–847. doi: 10.1016/j.scitotenv.2019.02.189

Zhao, J., Huang, S., Huang, Q., Wang, H., & Leng, G. (2018, September). Detecting the Dominant Cause of Streamflow Decline in the Loess Plateau of China Based onthe Latest Budyko Equation. *Water*, *10*(9), 1277. doi: 10.3390/w10091277

Zheng, Y., Huang, Y., Zhou, S., Wang, K., & Wang, G. (2018, December). Effect partition of climate and catchment changes on runoff variation at the headwater region of the Yellow River based on the Budyko complementary relationship. *Science of The Total Environment*, *643*, 1166–1177. doi: 10.1016/j.scitotenv.2018.06.195

Zveryaev, I. I. (2004). Seasonality in precipitation variability over Europe. *Journal of Geophysical Research: Atmospheres*, *109*(D5). doi: 10.1029/2003JD003668